Available online at www.sciencedirect.com
SCIENCE DIRECT®
Journal of the European Ceramic Society 25 (2005) 891–897
www.elsevier.com/locate/jeurceramsoc

Studying morphological characteristics of thermally treated bioactive glass ceramic using image analysis

C. Pritsos [a], E. Kontonasaki [a], X. Chatzistavrou [b], L. Papadopoulou [c], F. Pappas [a], P. Koidis [a], K. M. Paraskevopoulos [b,*]

[a] *School of Dentistry, Department of Fixed Prosthesis and Implant Proshtodontics, Aristotle University of Thessaloniki, 54124 Thessaloniki, Greece*
[b] *Physics Department, Aristotle University of Thessaloniki, 54124 Thessaloniki, Greece*
[c] *Department of Geology, Aristotle University of Thessaloniki, 54124 Thessaloniki, Greece*

Received 16 November 2003; received in revised form 30 March 2004; accepted 3 April 2004
Available online 20 June 2004

Abstract

Bioactive glass ceramics are materials which develop a strong bond with living tissues through a carbonate-containing hydroxyapatatite layer, similar to that of bone. Recently, the use of thermally treated bioactive glass in dental restorations has been proposed, as it could provide a bioactive surface, which in combination with a tissue regenerative technique could lead to periodontal tissues attachment. The purpose of this study was the investigation of the qualitative and quantitative alterations of thermally treated bioactive glasses after incubation in simulated body fluid (SBF) for different time intervals, through the use of Image Analysis methods. There is a remarkable decrease in the dimensions of bioactive glass particles—their shape being more elongated—with the immersion time in SBF and the depth from the surface. The influence on particles morphology in deeper layers is recognizable and the species in the coating, present bioactivity on the surface and in the volume.

Keywords: Electron microscopy; Optical microscopy; Glass ceramics; Biomedical applications; Image analysis

1. Introduction

Despite the well-documented bond formation between bioactive glasses and living tissues,[1–6] and their extended clinical use in orthopedics,[7] otolaryngology,[8] oral surgery[9] and periodontology[10,11], the potential of their attachment to soft periodontal tissues has received little investigation.

Tuominen et al.[12] observed the formation of hemidesmosomes of oral epithelial and connective tissues in contact to bioactive glass, while Kontonasaki et al.[13] reported that even with a considerable retardation, bioactive glass can still elicit bioactive behavior when coated on dental porcelain used in metal–ceramic restorations.

The formation of a well-bonded to the underlying bioactive glass–porcelain substratum hydroxycarbonate apatite layer, after immersion for various times in simulated body fluid (SBF)[14] evidenced the expression of bioactivity. The apatite layer was gradually formed in SBF by a continuous dissolution–reprecipitation process, leading initially in the formation of small calcium-phosphate crystals, which subsequently nucleated to apatite. The time for this nucleation varies depending on substratum crystallinity. Heat-treated Bioglass® has a varied degree of crystallinity and it was found that the nucleation on the smaller crystals—low degree of crystallinity and high surface energy—requires a smaller driving force or lower supersaturation than that for the induction of nucleation on a low-energy surface such as a well-crystallized surface.[15]

The knowledge of the condition in which bioactive glass particles are, as long as they are in contact to solutions that promote apatite formation, is crucial, as the bond between bone and bioactive materials largely depends on the rate of apatite formation on their surface,[16] which is in turn, related to the dissolution rate of bioactive glass in vitro.[17]

The way in which bioactive glass particles are gradually transformed through dissolution to apatite and the effect of their distance from surface has been investigated in some in vivo studies.[18–20] In these studies bioactive glass was not thermally treated which means that was mainly amorphous with little or no crystallinity.[21]

* Corresponding author. Tel.: +30 2310 998015; fax: +30 2310 994301.
E-mail address: kpar@auth.gr (K.M. Paraskevopoulos).

0955-2219/$ – see front matter © 2004 Elsevier Ltd. All rights reserved.
doi:10.1016/j.jeurceramsoc.2004.04.004

The aim of the present work was the quantitative study of the changes in the morphology (surface and volume changes) of bioactive glass particles of thermally treated bioactive glass coating applied on dental porcelain substrate, after its immersion in SBF for varying time periods.

2. Materials and methods

2.1. Specimen preparation

The materials used for the specimen preparation were dental porcelain IPS Classic (Margin, Ivoclar, Schaan, Liechtenstein) and bioactive glass (Bioglass 45S5), under the commercial name PerioGlas®. Ceramic disks with a diameter of 6 mm and a height of 1 mm were prepared as it is described analytically elsewhere[13] and exposed to the recommended thermal cycle, according to manufacturer' instructions (final $T = 950\,^{\circ}$C, heating rate $t = 80\,^{\circ}$C/min, vacuum). They were then coated with a specific pre-weighed amount of bioactive glass powder and exposed to a second thermal cycle ($T = 940\,^{\circ}$C, $t = 80\,^{\circ}$C/min, vacuum), since it was found that applying the particles to an already fired coating and using a second heat treatment particles adhesion could be promoted.

2.2. SEM-EDS and optical microscopy

Surface and in depth examinations were performed using the techniques of scanning electron microscopy (SEM) [(JEOL JSM 840-A) with associated energy dispersive spectroscopy (EDS) (EDS—Energy Dispersive Spectroscopy—Oxford ISIS-300)] and Optical Microscopy (Light Microscope Axiolab, Zeiss, Germany) with an attached CCD (SSC-DC58AP Color Video Camera, Sony Corporation, Japan) in order morphological and compositional variations of the developed apatite layer during different experimental conditions related to time to be determined. For the depth examination (cross-sectional study), the samples were embedded in an epoxy resin and were cut, vertical to the samples' surface.

2.3. Quantitative image analysis

The digital images were processed via image analysis software (Image Pro Plus 4.1, Media Cybernetics). For the statistical analysis One-Way Analysis of Variance (ANOVA) was used while homogeneity of groups was tested with Tukey's tests.

3. Results

The SEM image of an area of a characteristic heat treated sample with porcelain substrate coated with Bioglass and immersed in SBF for 30 days, is shown in Fig. 1. Bioglass particles and the surface layers of hydroxyapatite on their surface can easily be identified. In Fig. 1b and 1c the respective EDS spectra from the center of the particles and the surface layer are presented.

The images taken by Optical Microscope, are shown in Fig. 2. Also, the images after their processing for morphological image analysis are included.

The image analysis software allowed:

- The improvement of the images appearance, after images were transferred from the microscope to the computer workstation, while rendering them appropriate for calculations.
- The immediate comparison between two different areas of the specimens in order to reveal the different sum of particles.
- Fast and correct calculations, as the separation of particles from the rest of the specimen (background) was insured via image analysis.
- The immediate and automatic count of particles and the classification, by their size, in pre-chosen classes.

The measurements were performed throughout all layers of bioglass and the following parameters were calculated:

a. The major diameter of particles (Fig. 3a).
b. The minor diameter of particles (Fig. 3b).
c. The ratio of major to minor diameter of particles.
d. Mean diameter: the average length of the straight lines that connect two different points of particles outline and go through the weight center and that were measured per 2° (Fig. 3c).

The efficacy of the approach—use of longest and shortest lengths of various intersection shapes—has been tested in computer simulations of randomly oriented sections through the centers of ellipsoids and through randomly oriented ellipsoids distributed evenly in a sample volume above and below the section plane.[22–25]

In the surface of every specimen an area of 600 μm × 350 μm in the middle of the thickness of bioactive ceramic coating was studied. The percentage of the surface which the particles occupied was calculated at this area via image analysis (Table 1).

At the central part of every specimen an area of 440 μm thick and 480 μm deep from the surface of bioglass was chosen. The specific depth was chosen after several measurements so that this area did not exceed the bottom of bioglass coating. This area was divided to three parts, each 160 μm deep and was calculated the percentage of the surface covered by bioactive particles (Fig. 4). The results are shown in Table 2. In Tables 3–5, the results of statistical analysis are presented.

Results from the above analysis reveal a statistically significant reduction of the amount of bioglass particles in relation to both immersion time and distance from the exposed in SBF surface, but for the combined effect of these parameters the reduction was not statistically significant. This

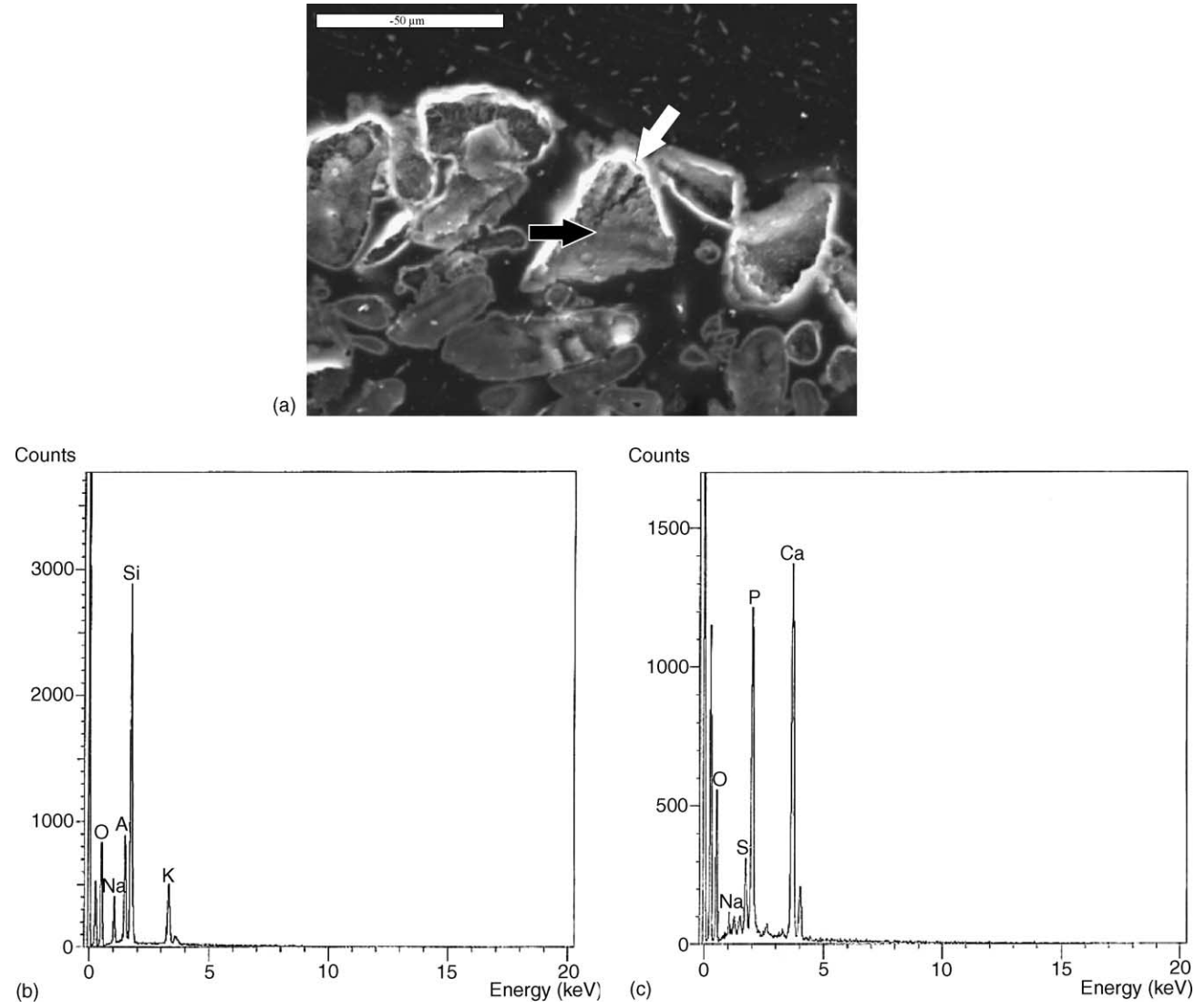

Fig. 1. (a) Heat treated sample coated with bioglass and immersed in SBF for 30 days. (b) EDS spectra from the center of the particles. (c) EDS spectra from the surface layer.

Table 1
Morphological characteristics of particles throughout all layers of Bioglass

	Major diameter (μm)	Minor diameter (μm)	Ratio of major to minor diameter	Mean diameter (μm)	Percentage occupied by the particles (%)
CB after 12 h	31.49	20.29	1.60	23.82	55
CB after 24 h	25.13	16.07	1.63	19.09	32
CB after 3 days	20.19	11.94	1.80	14.89	21
CB after 7 days	20.06	11.77	1.75	14.75	29
CB after 11 days	16.91	10.24	1.72	12.70	22
CB after 30 days	15.06	8.29	1.8	10.97	16

reduction remains significant from the first few hours to even 30 days immersion time.

4. Discussion

A significant transformation of the bioactive ceramic particles was evidenced not only on the exposed to SBF surface but even in deeper layers. The dimensions of the particles were reduced as the duration of the incubation in SBF increased and at the same time their shape became more elongated.

The dependence of mean bioactive glass particles surface on immersion time is presented in Fig. 5 where results from the quantitative image analysis are given. From this depen-

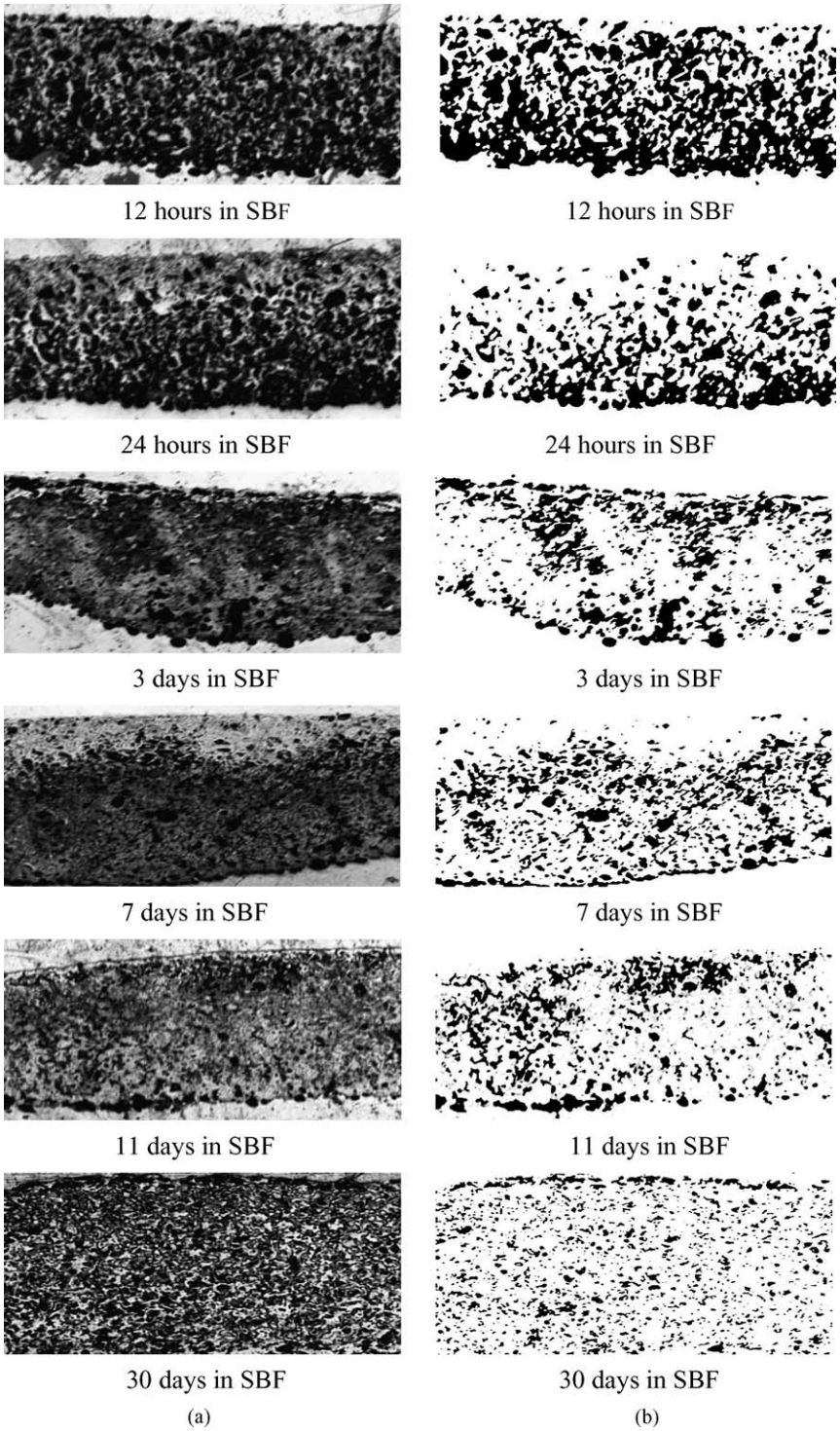

Fig. 2. Digital images before and after image analysis. (a) Images as taken by microscope. (b) Images after processing via image analysis software.

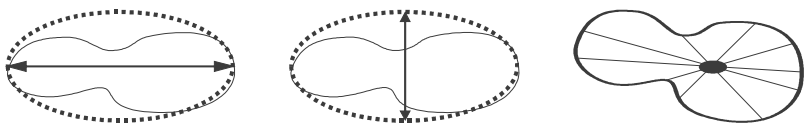

Fig. 3. Major diameter of particles (a), minor diameter (b), mean diameter (c).

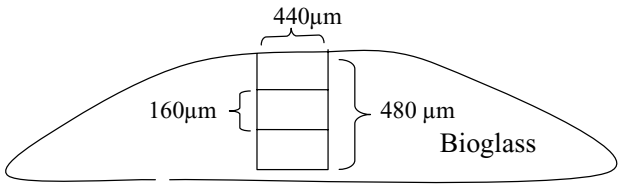

Fig. 4. Three layers (upper, mid and lower) of bioglass.

Table 2
Characteristics of bioactive glass particles in each layer

Area	Specimen	*n*	Mean $(\mu m)^2$
Upper layer (0–160 μm)	12 h	56	568.64
	24 h	27	350.07
	3 days	90	256.31
	7 days	45	156.36
	11 days	99	147.96
	30 days	74	196.92
Mid layer (161–320 μm)	12 h	71	534.08
	24 h	59	385.29
	3 days	86	218
	7 days	95	268.38
	11 days	86	183.67
	30 days	95	90.86
Lower layer (321–480 μm)	12 h	59	700.07
	24 h	64	546.75
	3 days	50	285.28
	7 days	79	233.67
	11 days	74	190.05
	30 days	93	100.73

Table 3
Results of ANOVA with which, the effect of immersion time in SBF on bioglass surface in association to the distance of bioglass particles from the exposed to the solution surface, was investigated

Source	ANOVA Bioactive glass particles' surface (μm^2)				
	Sum of squares	d.f.	Mean square	*F*	*P*
Corrected model	36270728	17	2133572	14.672	0.001
Intercept	1.06E+08	1	1.06E+08	728.278	0.001
Specimen	31354519	5	6270904	43.124	0.001
Area	1061658	2	530828.9	3.65	0.026
Specimen ×area	2578716	10	257871.6	1.773	0.061
Error	1.87E+08	1302	145416.6		
Total	3.24E+08	1301			

Table 4
Tukey's tests for bioactive glass surface homogeneity of different groups of specimens

	Groups			
	1	2	3	4
30 days	+			
11 days	+	++		
7 days		++		
3 days		++		
24 h			+++	
12 h				++++

Table 5
Tukey's tests for bioactive glass surface homogeneity of different areas within the same specimens

Groups	
Upper layer (0–160 μm)	+
Mid layer (161–320 μm)	+
Lower layer (321–480 μm)	+

dence, it is obvious that there is a decrease in the mean particle surface that follows a characteristic exponential profile in each layer.

In the three layers from the surface—upper, mid and lower—, the experimental results are well-fitted by the exponential model according to the relation

$$S = A\,e^{-at} + S_0$$

where *S* being the mean particle surface area; *t*, immersion time and α the exponential factor. The value of this factor α is representative of how quickly the phenomenon proceeds in each layer. Its value is decreased from the surface to the lower layer ($\alpha_{surface} = 1.46\ day^{-1}$, $\alpha_{mid} = 1.00\ day^{-1}$, $\alpha_{lower} = 0.57\ day^{-1}$) suggesting a retardation of the SBF influence with the depth.

Following the introduction of a bioactive ceramic to SBF, a partial dissolution of the surface is taking place

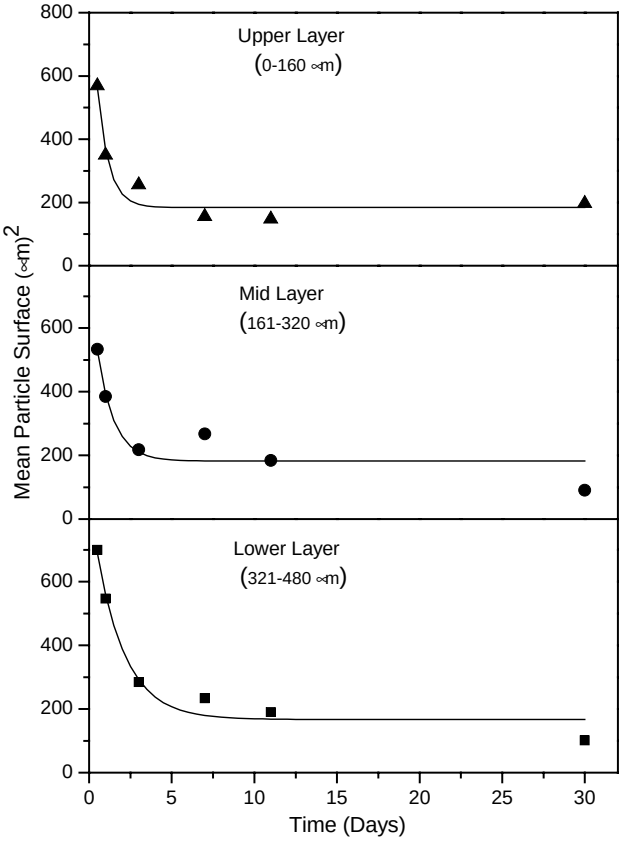

Fig. 5. The dependence of the mean particle surface on the immersion time in SBF.

resulting in the release of Ca^{2+}, HPO_4^{2-} and PO_4^{3-}, increasing the supersaturation of SBF in respect to apatite. A hydroxy-carbonate apatite layer (HCAp) can then be formed by the calcium and phosphate ions uptake from solution and by the incorporation of other electrolytes.[24] The bioactive behavior of these glasses depends on the cation diffusion for the development of a HCA layer, and such diffusion is related to the chemical structure of the glass (cation environment).[25] In more details, the mechanism responsible for HCA formation is the cation exchange between the bioactive glass surface and the aqueous environment (i.e., Ca^{2+}, Na^+ with H^+/H_3O^+), which involves a pH excursion from de-alkalization. Loss of soluble silica of silicic acid will then occur due to the breaking up of the silicate network (Si–O–Si) that also contributes to a change in pH. This is the reason for the reduction of bioglass particles dimensions after immersion in the solution, as the role of sodium in 45S5 Bioglass® is that of network modifier and it takes no part in the nucleation and growth of a HCAp layer and although calcium release is also reduced, it is retained as part of the amorphous calcium phosphate layer. Further dissolution results in the mass transport of calcium from the center of the particulate glass through the silica rich layer into the aqueous media, causing a reduction in the rate of dissolution. This effect is more pronounced for larger particle sizes.[20]

Results of this study revealed a significant interaction of the inner bioglass particles with SBF although they were not in contact with the solution. This was caused by solution penetration in the interior parts of bioglass coating through surface cracks which are consistently observed in the coatings when the inter-particle spacing is smaller than the particle diameter. For coatings with Bioglass® particles, sodium calcium silicate ($Na_2Ca_2Si_3O_9$) is crystallized on the surfaces of the coatings, as was evidenced by FTIR.[26,27] Following the specific thermal cycle for bioactive glass coatings preparation,[13] the degree of crystallinity was estimated higher than 60%, as reported by Filho et al.[21] Crystallization and stress generation due to thermal expansion coefficient mismatch[28,29] limit the maximum concentration and size of the embedded particles.[26]

EDS analysis confirmed that in regions where the particles of bioactive glasses were dissolved (outer parts of each particle), the Ca/P ratio ranged from 1.6 to 1.8, a value corresponding to non-stoichiometric biological apatite (calcium-deficient apatite).[30] The rate-controlling process of this Ca–P layer can change depending upon particle size, solution concentration and surface properties of the crystallites.[31]

Particle size is a factor influencing the reaction rate and particles of different size present different behavior under the same conditions, as it is considered that different particle sizes might bring in the factor of surface morphology, which has great influence on the reaction rate.[31] Large bioglass particles cause a greater and more rapid increase in pH from Si and Na exchange with H^+ from the solution resulting in higher Ca and P uptake and a faster HCAp formation.[32] The Ca adsorption and consequently HCAp formation rate is slower for the smaller particles. This may be attributed to physical differences such as the radius of curvature and surface roughness.[32]

The specific surface area is not the only factor that may affect the reaction behavior of various HA powders-the degree of crystallinity can probably play an important role in the reaction rate.[31] As has been reported, the earliest the precipitation of Ca and P in SBF the shorter the time necessary to block further ion exchange, dissolution and silica gel layer formation on bioglass, and thus the slower the surface reaction stages leading to HCAp formation.[33] In the present study bioglass coatings were substantially crystallized compared to non-thermally treated bioglass[27,34] and in this way silica network dissolution required more time to take place and as a result solution had more time to diffuse in the inner parts of the coatings, before hydroxycarbonate apatite sealed the reacting bioglass particles.

A dense HCAp layer covering the surface of bioactive glass coating was formed after 3 days in SBF[34] slowing down further ion exchange between bioactive glass particles and solution, thus inhibiting the complete transformation of the inner particles to HCAp. From that point forward any possible increase of the HCAp layer thickness occurs through nucleation and growth of the already formed apatite crystals.[34]

5. Conclusions

The bioactive glass particle dimensions decreased during the immersion in SBF and at the same time their shape became more elongated. A significant transformation of the bioactive ceramic particles was obvious not only on the exposed to SBF surface but even in deeper layers. Bioglass coatings crystallization upon heat treatment, through a dual mechanism of: (a) surface cracks formation and (b) retardation of silica network dissolution of the outer bioglass particles resulting in increased time for solution–particles interactions, may be responsible for these observations.

Acknowledgements

The authors wish to thank Omega Trading (Greek representative) for the supply of PerioGlas®.

References

1. Hench, L. L., Splinter, R. J., Allen, W. C. and Greenlee, T. K., Bonding mechanism at interface of ceramic prosthetic materials. *J. Biomed. Mater. Res. Symp.* 1971, **2**, 117–141.
2. Kokubo, T., Shigematsu, M., Nagashima, Y., Tashiro, M., Nakamura, T., Yamamuro, T. and Higashi, S., Apatite- and wallastonite-containing

glass ceramics for prosthetic application. *Bull. Inst. Chem. Res. Kyoto Univ.* 1982, **60**, 260–268.
3. Wang, S. A., Chen, A. Y., Yu, Z. E., Huang, Z. J. and Wao, Y. M., Alveolar ridge augmentation with bioactive glass ceramics: a histological study. *J. Oral. Rehabil.* 1989, **16**(3), 229–239.
4. Andersson, O., Karlsson, K. and Kangasniemi, K., Calcium phosphate formation at the surface of bioactive glass in vivo. *J. Non-Cryst. Solids* 1990, **112**, 290–296.
5. Ohura, K., Nakamura, T., Yamamuro, T., Kokubo, T., Ebisawa, Y., Kotoura, Y. and Oka, M., Bone-bonding ability of P_2O_5-free $CaO{\cdot}SiO_2$ glasses. *J. Biomed. Mater. Res.* 1991, **25**(3), 357–365.
6. Nakamura, T., Senaha, Y., Kitsugi, T., Kokubo, T., Ebisawa, Y., Kotura, Y., Oka, M. Augmentation of bonding of porous-coated materials to bone with bioactive ceramic granules. In *Bioceramics, Vol 7*, ed. O. Andersson, R. Happonen and A. Yli-Urpo. Butterworth-Heinemann Ltd., Turku, Finland, 1994, pp. 145–149.
7. Gummel, J., Zippel, H. and Hahnel, H., Replacement of the lumbar vertebral bodies with machinable bioactive glass ceramic. *Z. Klin. Med.* 1988, **43**, 1971–1973.
8. Merwin, G. E., Review of bioactive materials for otologic and maxillofacial application. In *Handbook of Bioactive Ceramic*, ed. T. Yamamuro, L. L. Hench and J. Wilson. CRC Press, Boca Raton, FL, 1990, pp. 323–328.
9. Wilson, J., Clark, A. E., Douek, E., Krieger, J., King, S. W. and Saville, Z. J., Clinical applications of bioglass implants. In *Bioceramics. Vol 7*, ed. O. Andersson, R. Happonen and A. Yli-Urpo. Butterworth-Heinemann Ltd., Turku, Finland, 1994, pp. 415–422.
10. Zamet, J. S., Darbar, U. R., Griffiths, G. S., Bulman, J. S., Bragger, U., Burgin, W. and Newman, H. N., Particulate bioglass as a grafting material in the treatment of periodontal intrabony defects. *J. Clin. Periodontol.* 1997, **24**, 410–418.
11. Oonishi, H., Kushitani, S., Yasukawa, E., Iwaki, H., Hench, L. L., Wilson, J., Tsuji, E. and Sugihara, T., Particulate bioglass compared with hydroxyapatite as a bone graft substitute. *Clin. Orthop.* 1997, **334**, 316–325.
12. Tuominen, U., Salonen, J., Haponnen, R. and Yli-Urpo, A., Attachment of human oral mucosa to bioactive glass in vitro. In *Bioceramics, Vol 6*, ed. P. Ducheyne and D. Christiansen. Butterworth-Heinemann Ltd., Philadelphia, 1993, pp. 151–156.
13. Kontonasaki, E., Papadopoulou, L., Zorba, T., Paulidou, E., Paraskevopoulos, K. and Koidis, P., Apatite formation on dental ceramics modified by a bioactive glass. *J. Oral Rehabil.* 2003, **30**, 893–902.
14. Kokubo, T., Kushitani, H., Sakka, S., Kitsugi, T. and Yamamuro, T., Solutions able to reproduce in vivo-surface structure changes in bioactive glass-ceramic A-W3. *J. Biomed. Mater. Res.* 1990, **24**, 721–734.
15. Clupper, C. D., Mecholsky, Jr. J.J., LaTorre, P. G. and Greenspan, C. D., Bioactivity of tape cast and sintered bioactive glass-ceramic in simulated body fluid. *Biomaterials* 2002, **23**, 2599–2606.
16. Fujiu, T., Ogino, M., Kariya, M. and Ishimura, T., New explanation of the bonding behavior of fluorine containing bioglass. *J. Non-Cryst. Solids* 1983, **56**, 417–422.
17. Hyakuna, K., Yamarnuro, T., Kotoura, Y., Oka, M., Nakamura, T., Kitsugi, T., Kokubo, T. and Kushitani, H., Surface reactions of calcium phosphate ceramics to various solutions. *J. Biomed. Mater. Res.* 1990, **24**(4), 471–488.
18. MacNeill, S. R., Cobb, C. M., Rapley, J. W., Glaros, A. G. and Spencer, P., In vivo comparison of synthetic osseous graft materials. A preliminary study. *J. Clin. Periodontol.* 1999, **26**(4), 239–245.
19. Vogel, M., Voigt, C., Gross, U. M. and Muller-Mai, C. M., In vivo comparison of bioactive glass particles in rabbits. *Biomaterials* 2001, **22**, 357–362.
20. Pryce, S. R. and Hench, L. L., Dissolution characteristics of bioactive glasses. *Key Eng. Mater.* 2003, **240–242**, 201–204.
21. Filho, O. P., La Torre, G. P. and Hench, L. L., Effect of crystallization on apatite-layer formation of bioactive glass 45S5. *J. Biomed. Mater. Res.* 1996, **30**, 509–514.
22. Kellerhals, R., Shaw, J. and Arora, V. K., On grain size from thin sections. *J. Geol.* 1975, **83**, 79–96.
23. Peterson, T., A refined technique for measuring crystal size distributions in thin section. *Contrib. Miner. Petrol* 1996, **124**, 395–405.
24. Legeros, Z. R., *Calcium Phosphates in Oral Biology and Medicine*. Karger, 1991, pp. 82–107.
25. Arcos, D., Greenspan, C. D. and Vallet-Regi, M., Influence of the stabilization temperature on textural and structural features and ion release in SiO_2–CaO–P_2O_5 sol–gel glasses. *Chem. Mater.* 2002, **14**, 1515–1522.
26. Gomez-Vega, J. M., Saiz, E., Tomsia, A. P., Marshall, G. W. and Marshall, S. J., Bioactive glass coatings with hydroxyapatite and Bioglass® particles on Ti-based implants. *1. Processing. Biomater.* 2000, **21**, 105–111.
27. Chatzistavrou, X., Zorba, T., Kontonasaki, E., Chryssafis, K., Koidis, P. and Paraskevopoulos, K., Following bioactive glass behavior beyond melting point by thermal and optical methods. *Phys. Stat. Sol. (a)* 2004, **201**, 944–951.
28. Krajewski, A., Ravagliori, A., De Portu, G. and Visani, R., Physicochemical approach to improving adherence between steel and bioactive glass. *Am. Ceram. Bull.* 1985, **64**, 679–683.
29. Khajotia, S. S., Mackert, J. R., Twiggs, S. W., Russell, C. M. and Williams, A. L., Elimination, via high-rate laser dilatometry, of structural relaxation during thermal expansion measurement of dental porcelains. *Dent. Mater.* 1999, **15**, 390–396.
30. LeGeros, R. Z., Biologically relevant calcium phosphates: preparation and characterization. In *Calcium Phosphates in Oral Biology and Medicine*. Karger, 1991, pp. 4–24.
31. Shi, D., Jiang, G. and Bauer, J., The effect of structural characteristics on the in vitro bioactivity of hydroxyapatite. *J. Biomed. Mater. Res. (Appl. Biomater.)* 2002, **63**, 71–78.
32. Greenspan, D. C., Zhong, J. P. and LaTorre, G. P., Effect of surface area to volume ratio on in vitro surface reactions of bioactive glass particulates. In *Proceedings of the 7th International Symposium on Ceramics in Medicine, Bioceramics, Vol 7*, ed. Ö. -H. Anderrson and A. Yli-Upro. Butterworth-Heinemann Ltd., Turku, Finland, 1994, pp. 55–60.
33. Zhong, J. P. and Greenspan, D. C., Bioglass surface reactivity: from in vitro to in vivo. In *Proceedings of the 11th International Symposium on Ceramics in Medicine, Bioceramics, Vol 11*, ed. R. Z. LeGeros, and J. P. LeGeros. World Scientific Publishing Co. Pte. Ltd., New York, USA, 1998, pp. 415–418.
34. Papadopoulou, L., Kontonasaki, E., Zorba, T., Chatzistavrou, X., Pavlidou, E., Paraskevopoulos, K., Sklavounos, S. and Koidis, P., Dental ceramics coated with bioactive glass: surface changes after exposure in a simulated body fluid under static and dynamic conditions. *Phys. Stat. Sol. (a)* 2003, **198**, 65–75.